

## Supporting Information

### Field supported slow magnetic relaxation in quasi-one-dimensional copper(II) complex with a pentaheterocyclic triphenodioxazine

D.V. Korchagin,<sup>\*a</sup> E.P. Ivakhnenko,<sup>b</sup> O.P. Demidov,<sup>c</sup> A.V. Akimov,<sup>a</sup> R.B. Morgunov,<sup>a</sup> A.G. Starikov,<sup>b</sup> A.V. Palii,<sup>a</sup> V.I. Minkin,<sup>b</sup> and S.M. Aldoshin<sup>a</sup>

<sup>a</sup> *Institute of Problems of Chemical Physics, Russian Academy of Sciences, 1 Acad. Semenov Av., 142432 Chernogolovka, Russia; korden@icp.ac.ru*

<sup>b</sup> *Institute of Physical and Organic Chemistry, Southern Federal University. 194/2 Stachki St. 344090 Rostov on Don. Russia*

<sup>c</sup> *North Caucasus Federal University. 1 Pushkin st., Stavropol, Russian Federation, 355017*

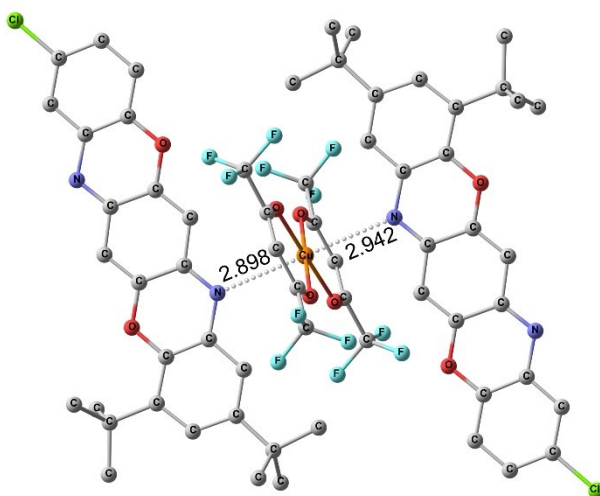


**Fig. S1.** Geometry characteristics of monomeric fragment of coordination polymer **I** calculated by the DFT (B3LYP/6-311++G(g,p)) method. Bond lengths are given in Å, hydrogen atoms are omitted for clarity.

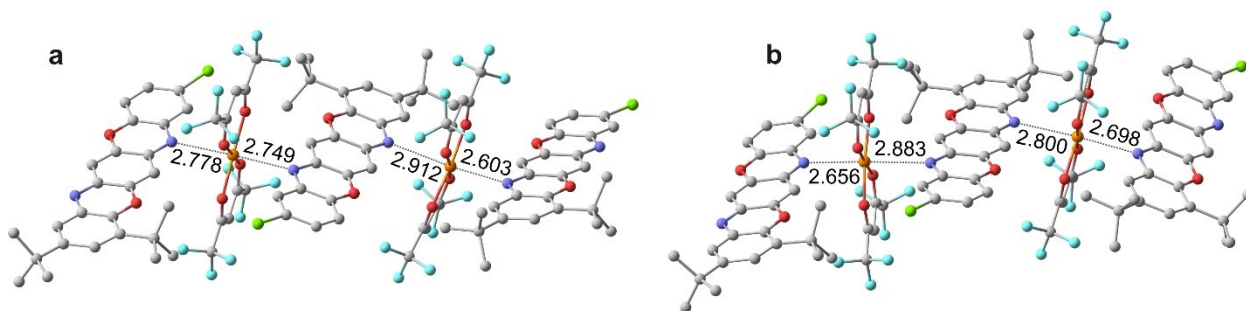


**Fig. S2.** Optimized geometries of dimer fragments of **I** calculated at B3LYP/Def2-SVP level. Bond lengths are given in Å, hydrogen atoms are omitted for clarity.

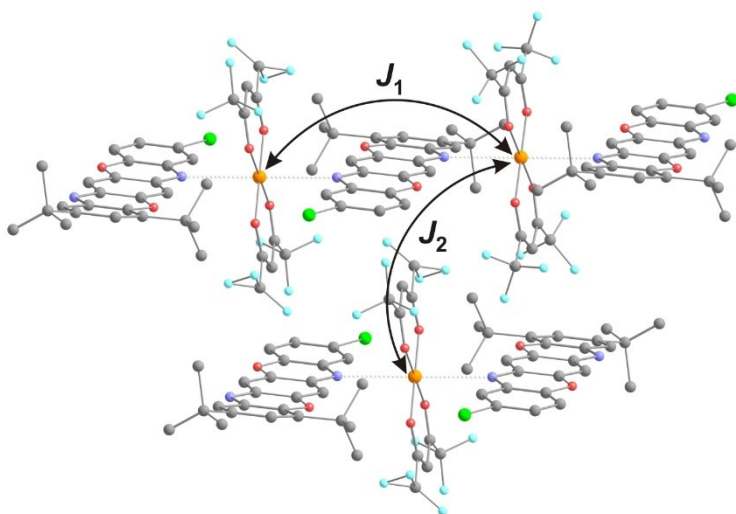


**Fig. S3.** Possible Cu-Cu exchange coupling channels in **I**.

**Table S1.** The exchange spin coupling parameters ( $J$ ,  $\text{cm}^{-1}$ ) calculated by the DFT method.

Approximation	$*J_1$	$J_2$	$J_3$
B3LYP/def2-SVP	0.42	0.21	0.42
B3LYP/def2-TZVP	-0.01	-0.01	-0.01
TPSSh/def2-TZVP	0.18	0.09	0.18

\*Formulas for the calculation  $J_1$ - $J_3$ .

$$J_1 = -(E_{\text{HS}} - E_{\text{BS}}) / S_{\text{max}}^2, [1].$$

$$J_2 = -(E_{\text{HS}} - E_{\text{BS}}) / (S_{\text{max}} * (S_{\text{max}} + 1)), [2].$$

$$J_3 = -(E_{\text{HS}} - E_{\text{BS}}) / (\langle S^2 \rangle_{\text{HS}} - \langle S^2 \rangle_{\text{BS}}), [3].$$

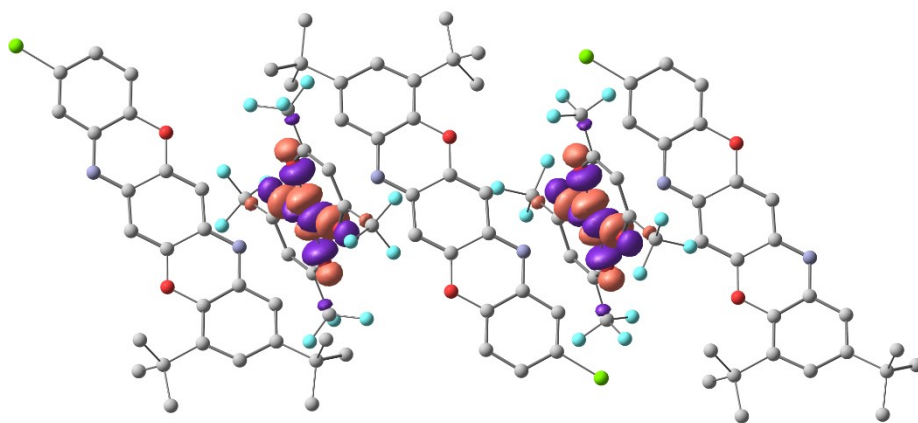


**Fig. S4.** Single-occupied natural (magnetic) orbital in dimer fragment of **I**.

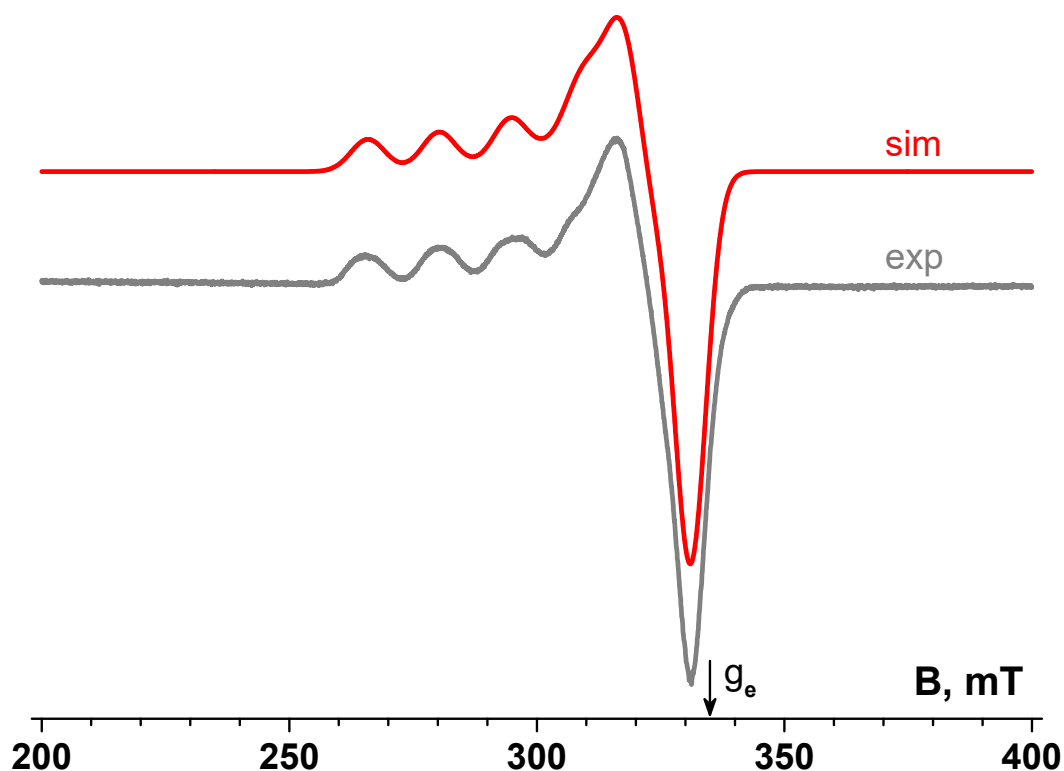


**Fig. S5.** Solid state EPR spectra for **I** (gray line) collected at 7 K and simulated EPR spectra for  $S=1/2$ ,  $g_{\perp} = 2.0639$ ,  $g_{\parallel} = 2.3332$ ,  $A(^{65}\text{Cu}) = [84.5; 84.5; 459]$  MHz (red line), linewidth 6.6 G. Microwave frequency 9.385423 GHz

**Table S2.** The DFT calculated principle values of g-tensor for monomeric fragment of **I**.

Level of theory	g-Tensor		
	x	y	z
B3LYP def2-SVP	2.055	2.057	2.179
B3LYP def2-TZVP	2.057	2.058	2.190
TPSSH def2-SVP/QZVPP*	2.046	2.047	2.149
TPSSH def2-TZVP/QZVPP*	2.046	2.047	2.147
ZORA TPSSH def2-SVP/QZVPP*	2.047	2.048	2.152

ZORA TPSSH def2-TZVP/QZVPP*	2.047	2.048	2.150
ZORA D3 TPSSH def2-SVP/QZVPP*	2.047	2.048	2.152
D3 TPSSH def2- TZVP/QZVPP*	2.049	2.050	2.157

\* QZVPP basis set was used for copper atom

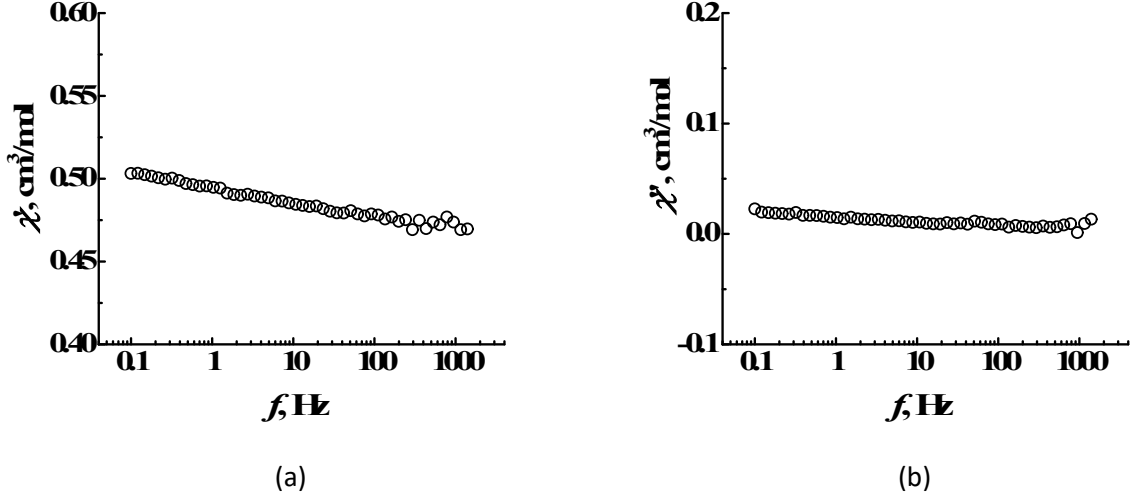


Fig. S6. Frequency dependence of the in-phase  $\chi'$  (a), out-of-phase  $\chi''$  (b) AC susceptibility  $\chi_M$  at temperature  $T = 2\text{K}$  and  $H_{DC} = 0\text{ Oe}$ .

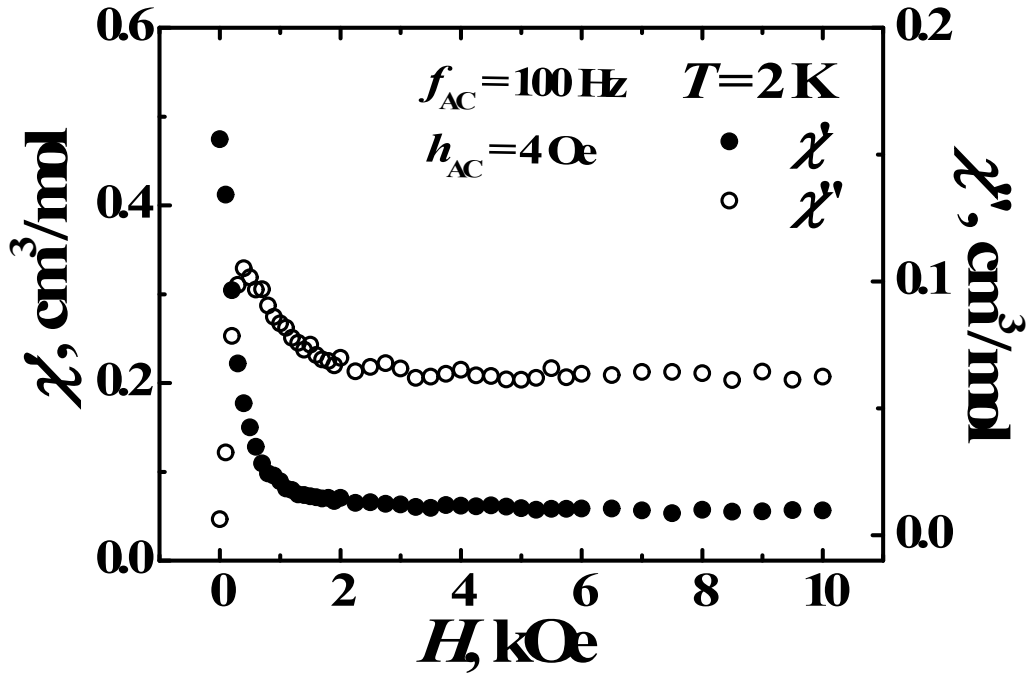
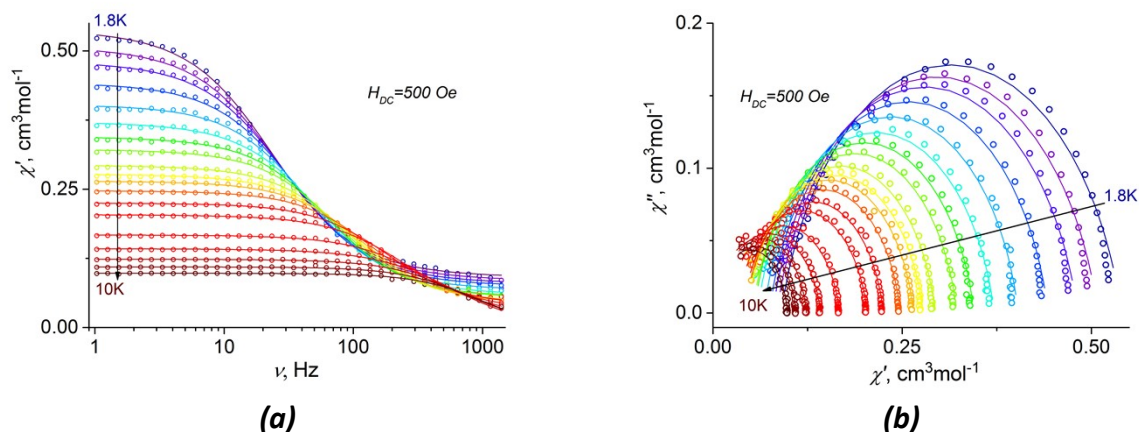


Fig. S7. Field dependence of the in-phase  $\chi'$  and out-of-phase  $\chi''$  AC susceptibility  $\chi_M$  at temperature  $T = 2\text{K}$  and frequency  $f_{AC} = 100\text{ Hz}$ . The maximum on the out-of-phase  $\chi''$  AC susceptibility is at  $H_{DC} \sim 500\text{ Oe}$ .



**Fig. S8.** Frequency dependence of the in-phase  $\chi'$  (a) AC susceptibility  $\chi_M$  and Cole-Cole diagrams (b) at different temperatures and  $H_{DC}=500$  Oe for **I** (points – experiment, lines – fit by generalized Debye model).

**Table S3.** Best fit parameters of the one-component Debye model for the Cole-Cole plot of complex **I** at  $H_{DC} = 500$  Oe

$T, K$	$\chi_S, \text{cm}^3 \text{mol}^{-1}$	$\chi_T, \text{cm}^3 \text{mol}^{-1}$	$\tau, s$	$\alpha$	$R_1^a$
1.8	0.090	0.540	0.679E-02	0.171	0.32E-02
1.9	0.084	0.509	0.604E-02	0.167	0.30E-02
2.0	0.079	0.482	0.537E-02	0.161	0.31E-02
2.2	0.074	0.443	0.451E-02	0.148	0.19E-02
2.4	0.068	0.403	0.366E-02	0.136	0.20E-02
2.6	0.059	0.372	0.299E-02	0.144	0.15E-02
2.8	0.054	0.345	0.253E-02	0.134	0.15E-02
3.0	0.052	0.322	0.217E-02	0.128	0.93E-03
3.3	0.046	0.293	0.173E-02	0.125	0.12E-02
3.5	0.045	0.277	0.153E-02	0.125	0.10E-02
3.7	0.042	0.265	0.133E-02	0.121	0.61E-03
4.0	0.043	0.247	0.113E-02	0.115	0.45E-03
4.5	0.039	0.225	0.867E-03	0.121	0.54E-03
5.0	0.031	0.204	0.655E-03	0.129	0.42E-03
6.0	0.020	0.167	0.441E-03	0.129	0.44E-03
7.0	0.005	0.142	0.291E-03	0.143	0.31E-03
8.0	0.001	0.123	0.237E-03	0.108	0.221E-03
9.0	0.004	0.110	0.202E-03	0.090	0.25E-03
10.0	0.000	0.098	0.163E-03	0.074	0.24E-03

<sup>a</sup> The mean residual sum of squares,  $R_1 = \frac{1}{n} \sum_{i=1}^n \frac{(Y_{\text{exp}} - Y_{\text{calc}})^2}{Y_{\text{exp}}^2}$

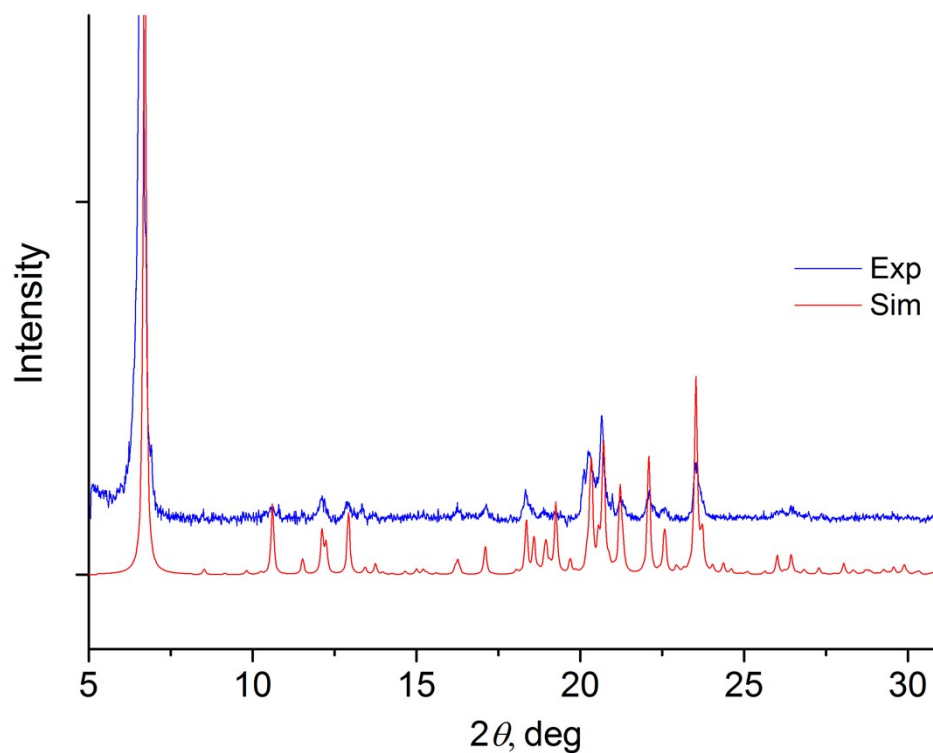


**Fig. S9.** Powder X-ray diffraction pattern of polycrystalline sample of complex I: experimental (blue), and calculated from single crystal data (red).

### References

1. A. P. Ginsberg, *J. Am. Chem. Soc.*, 1980, **102**, 111-117.
2. A. Bencini, D. Gatteschi, *J. Am. Chem. Soc.*, 1980, **108**, 5763-
3. T. Soda, Y. Kitagawa, T. Onishi, Y. Takano, Y. Shigeta, H. Nagao, Y. Yoshioka, and K. Yamaguchi, *Chem. Phys. Lett.* 2000, **319**, 223-230.